Group 5

ANALYSIS OF DRAGONFLY INSPIRED FLAPPING WING MODEL

Design Project Report

Aerodynamics Lab II (AE39001)
Autumn 2023

Prof. Sandeep Saha

ABSTRACT:

The mechanism of lift generation by winged insects is an area of active research. Especially that by quad winged dragonflies. Various characteristics of flight such as the wingbeat frequency and phase difference between the wings are sure to affect the amount of lift and drag produced. We aim to explore experimentally how these parameters affect the flight performance. During flight, the wing of the dragonflies (or any insect for that matter) does not behave the same way in the downstroke as it does in the upstroke , as it will not be able to generate lift if it were so. Hence, in our model we let the wing rotate passively about an axis parallel to its span, so that the wing encounters maximum resistance on the downstroke and lesser resistance in the upstroke.

The study also involved assessing lift generated by wing pairs through force sensors affixed to the model. We analyzed the disparity in force during the upstroke and downstroke of the flapping wing. This was achieved by graphing force against time using the data from the force sensors. The difference in the maxima and minima obtained from this graph provides us a way to quantify the lift. Additionally, we investigated flow characteristics utilizing a smoke visualization setup, aiming to glean deeper insights into the aerodynamic behavior of the model.

INTRODUCTION:

Flapping wing aerodynamics is a captivating field at the intersection of biology and engineering, delving into the intricate mechanics behind the flight of various creatures, from insects like bees and dragonflies to small birds.

In this study we aim to develop a four winged flapping wing model (a pair of front and a pair of hind wings) based on dragonflies. Dragonflies unlike bees or butterflies have two pairs of wings with each pair flapping separately resulting in more aerodynamic lift and increased flight control inputs and stabilization techniques in different flight modes. As observed in nature, dragonflies control their forewing and hindwings independently by their powerful and complicated thorax muscles. As a result, the two pairs of wings employ different wing kinematics and relative phase angles during different flight modes.

BACKGROUND AND THEORY:

Several studies have been carried out on the kinematics of forward flight and hovering, using different kinds of techniques. In 1988, Azuma and Watanabe examined the free flight of a dragonfly to determine the flight performance at different flight speeds. Somps and Luttges experimentally demonstrated the effect of unsteady separated

flows and concluded that large lift forces are actually produced by unsteady flow-wing interaction.

A computational fluid dynamics (CFD) method was employed by Wang to study the vortex wake structure of a single airfoil and the aerodynamic forces involved with a hovering dragonfly. Time variation of the aerodynamic force in each flapping cycle and the vortex shedding process was examined. A large vertical force was created during each downstroke and the mean vertical force was enough to support the weight of a classic dragonfly. A vortex pair was created during each downstroke. The large vertical force was explained by the downward two dimensional (2D) jet induced by the vortex pair.

Lan and Sun used a CFD method on two airfoils to simulate dragonfly wing pair (i.e., forewing and hindwing) interaction in hovering flight. They compared these results with simulated flow on a single airfoil. The results of this single airfoil were similar to the flow structure and aerodynamic forces observed in both Wang's computation and Freymuth's experiment. They showed that the forewing and hindwing airfoils were flapping 180 out of phase with one another (counter-stroking). Although each airfoil generated aerodynamic forces that were similar to the single airfoil, their interaction caused the vertical forces (generated by each) to be reduced by 20%. Sun and Lan10 studied 3D aerodynamic interaction between the wing pairs of a Aeshna juncea dragonfly in hover flight, using a CFD method. They found that this large vertical force coefficient is caused by the leading edge vortex (LEV), associated with the delayed stall mechanism.

Wang presented via 2D computation that dragonfly-style hovering with a large stroke plane inclination (almost 60 deg) relies substantially on drag to produce vertical force. They also showed that this mode of hovering requires less power than a symmetrical horizontal stroke. Sun and Huang by employing numerical simulation discovered, at positive phase difference (gd) where hindwing leads forewing, the mean total thrust and mean total vertical force of the forewing and hindwing are only slightly affected by the forewing–hindwing interaction, while at negative gd (hindwing lags forewing), the forces, especially the mean total vertical force, are significantly reduced, compared with the case without interaction. The reason for the great reductions in the forces at negative gd is as follows: the forewing in each of its downstroke generates a downward ''jet'' behind it; when the hindwing lags the forewing, it moves in the jet and its effective angle-of-attack is significantly decreased, resulting in a large reduction in its aerodynamic force; this makes the reductions in the thrust and total vertical force.
Wang and Russell calculated the aerodynamic force and power of a tethered dragonfly as a function of the phase lag between the forewings and hindwings. They found that

out-of-phase movement (such as in steady hovering) uses minimal power to generate the required force to balance the weight, while in-phase movement (such as in take-off) provides additional force enabling the dragonfly to accelerate.

Hu et al. constructed a pair of dynamically scaled robotic dragonfly wings to investigate wing pair aerodynamic interaction. They systematically changed the forewing–hindwing phase difference and measured the resulting aerodynamic forces. In hovering flight (gamma = 0), the lift force generated by the wing pairs is very large. When gamma =180, the generated lifting forces were not as large but still sufficient to stabilize body posture and suspend vibrations. In nature, gamma = 180 is used by dragonflies in hovering mode, while gamma = 0 is normally used for accelerated flight. For forward flight, the wing–wing interaction decreased the hindwing lift while improving the forewing lift at all phase changes. Additionally, the total lift was slightly decreased as g was changed from 0 to 90. It considerably dropped (by 18%) at gamma = 270. These results correspond well with free-flight observations, which show that dragonflies normally use a phase difference of 50 to 100 for forward flight and seldom use gamma= 270.

Nagai et al. experimentally investigated the effect of the phase variation between the forewings and hindwings on a dragonfly's aerodynamic characteristics in forward flight as well as hovering. They demonstrated in forward flight that a phase advanced hindwing (ahead of the forewing), which is frequently used by dragonflies in steady flight, generates more lift at a greater efficiency than would occur without interaction between the wings. This is largely due to the benefits gained from downwash caused by the forewing.

MATERIALS:

Chrome Plated Steel Rods, Carbon Fiber Rods, DC Motor, Batteries, Stainless Steel Dowel Pins, Bevel gears, 3D Printed CAD Models(Refer to Appendix for the CAD files), Mylar sheet(50 micron), Thin Wire, Arduino Uno, Force Sensor, Soldering Iron.

CAD MODELS:

LINKS 1 & 2:

Fig 1

PASSIVE ROTATION JOINT: (Right and Left)

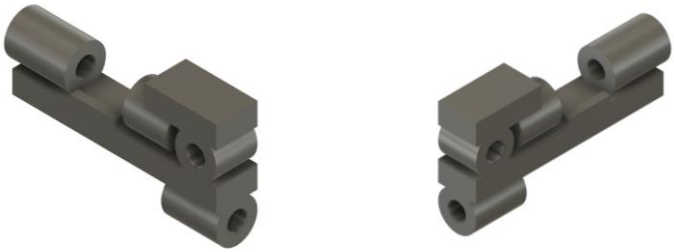

Fig 2

BASE: (different views)

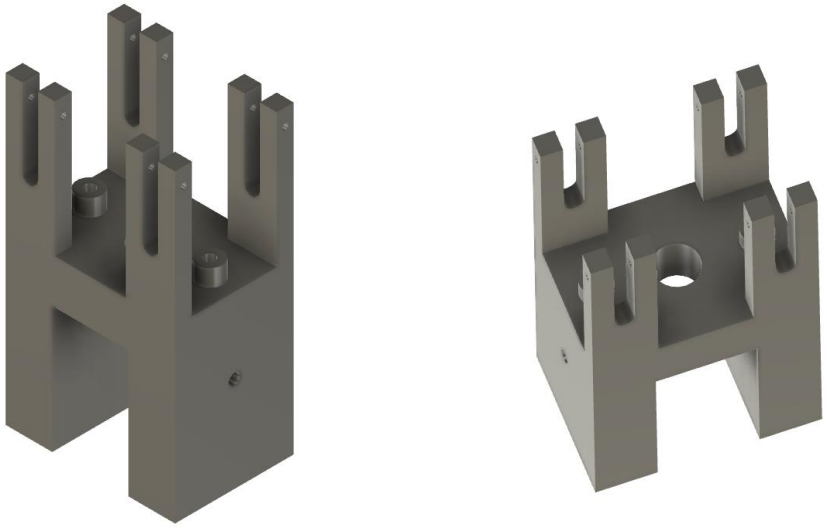

Fig 3

SLIDER:

Fig 4

ROTATING JOINT:

Fig 5

CALCULATION OF DIMENSIONS:

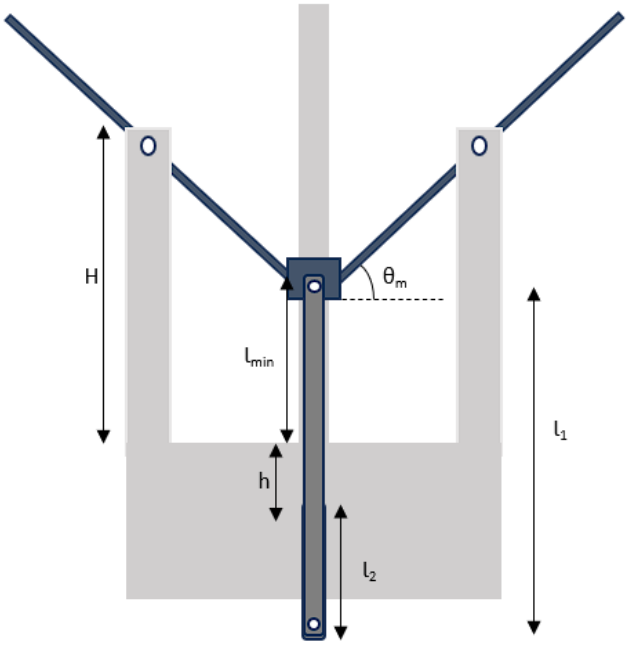

Fig 6 (Schematic of model at max positive angular amplitude)

θ_m = Maximum Angular Amplitude

$\boxtimes_{min} = \boxtimes_1 - \boxtimes_2 - h$

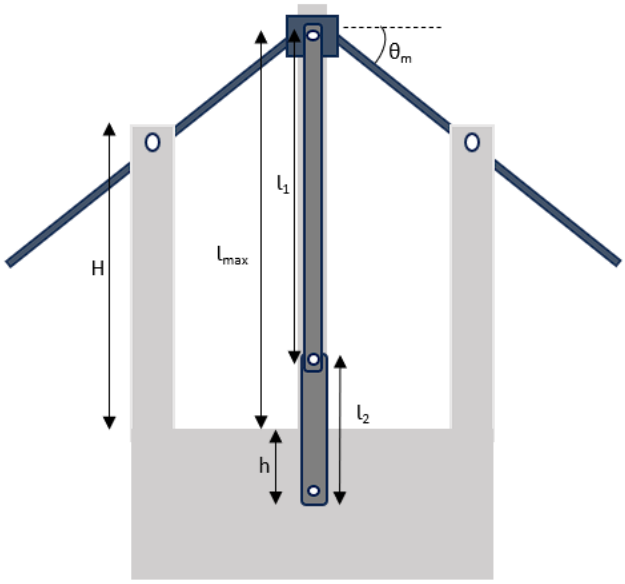

Fig 7 (Schematic of model at max negative angular amplitude)

$\boxtimes_{max} = \boxtimes_1 + \boxtimes_2 - h$

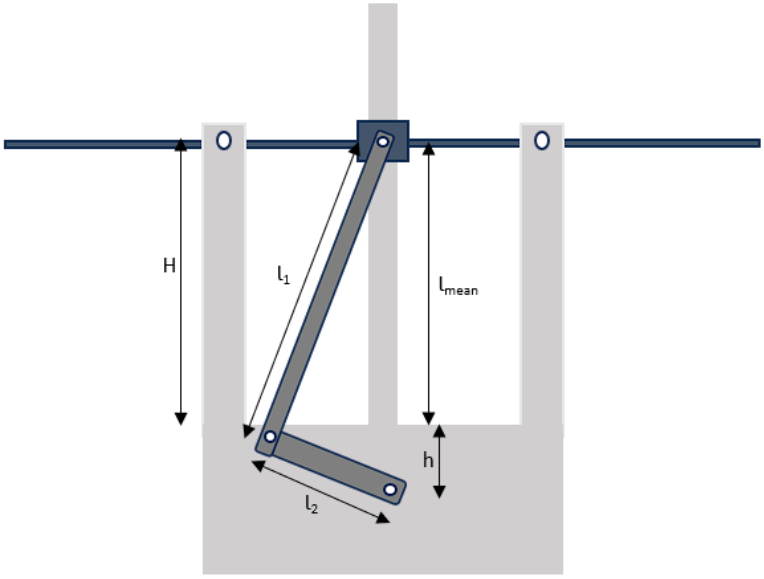

Fig 8 (Schematic of model at zero angular amplitude)

$$\boxtimes_{mean} = (\boxtimes_{max} + \boxtimes_{min})/2 = \boxtimes_1 - h$$
$$H = \boxtimes_{mean} = \boxtimes_1 - h$$

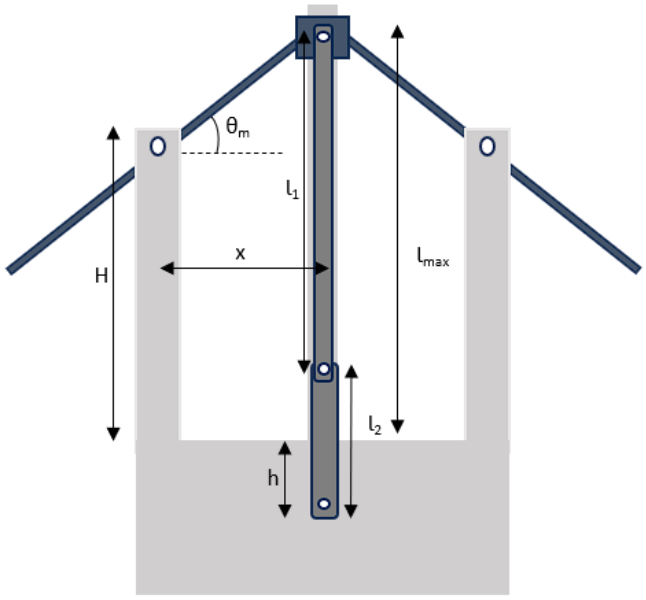

Fig 9 (Schematic of model at max negative angular amplitude for calculating x)

$$\tan(\theta_m) = (\boxtimes_{max} - H)/x = \boxtimes_2/x$$
$$\boxtimes_2 = x.\tan(\theta_m)$$

Deriving these relations, we have figured the required dimensions. Accounting for the error caused due to lateral shift of the connecting carbon fibers to the pin hole in the slider, we finalize the following dimensions:

$\theta_m = 60^o$

x = 30 mm

l_1 = 112.85 mm

l_2 = 38.5 mm

h = 44.35 mm

H = 68.5 mm

Remaining dimensions in the CAD model are decided in accordance with the dimensions of the rods and pins acquired.

WORKING OF MODEL:

Due to the presence of bevel gears, as the motor rotates, it imparts rotational motion to link 1 on each side. The interconnected links and slider then convert this rotational movement into vertical translational motion. Essentially, this mechanism mirrors the functionality of a slider-crank mechanism. The slider on each side executes an upward and downward motion, consequently driving the flapping motion of the wings.The phase difference can be changed by changing the initial orientation of link 1 on one side. The amplitude of the motion can be increased by changing the dimensions of link 1 and correspondingly changing the dimensions of the base and link 2.

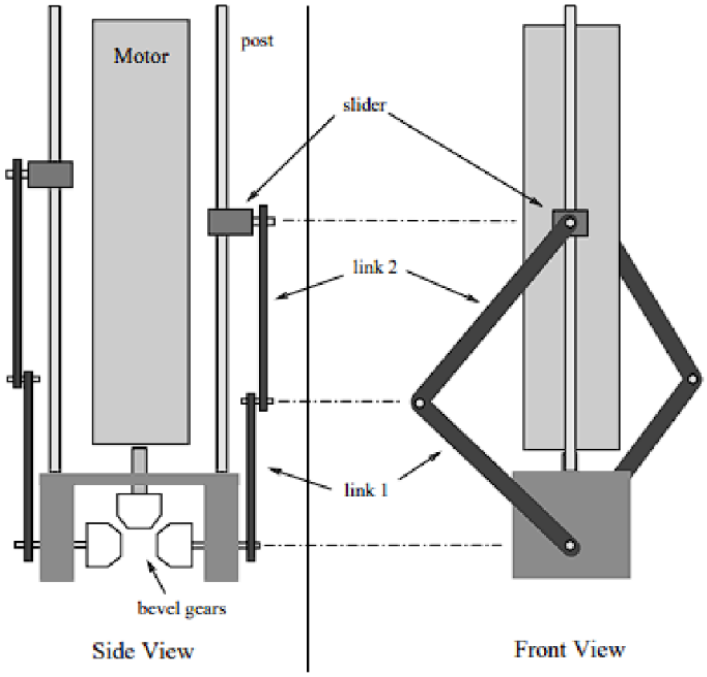

Fig 10 (gear mechanism)

Facilitating this motion is a passive rotation joint that enables the wing to revolve around the rod connecting it to the slider. It's worth noting that this rotational capability is constrained, limited to approximately 90 degrees of movement.

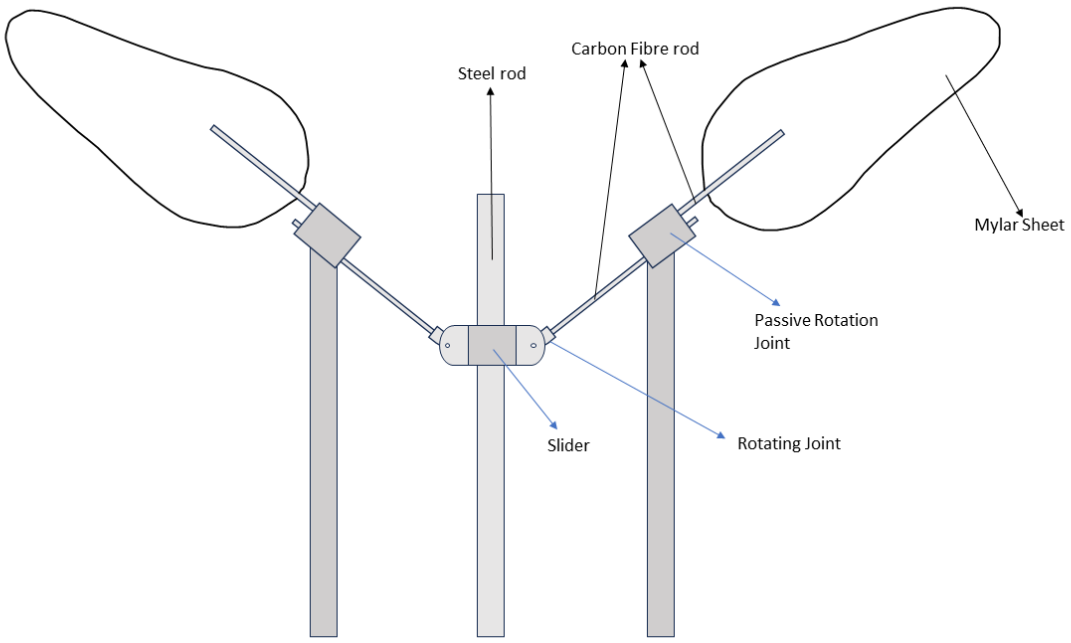

Fig 11 (Front view of the slider mechanism)

FINAL DESIGN:

- We incorporated 2 pairs of wings that are powered by a single DC motor. We achieved this using a DC motor driven double slider mechanism involving the use of bevel gears. The amplitude (angle) of the wing's flapping motion can be varied by adjusting the lengths of the link 1 and link 2. Phase difference is being introduced between the front and hind wing pairs by changing the initial positions of the slider of front wing and hind wing pairs.
- The wing is designed such that it is allowed to passively rotate. This is achieved by making the wing out of a thin mylar film and providing a passive rotation joint that allows the wing to rotate under an angle constraint.
- We calculated the lift generated by the pairs of wings using force sensors that were attached to the model. Simultaneously, a smoke visualization setup was used to gain insights into the aerodynamics of the model.

RESULT AND DISCUSSION:

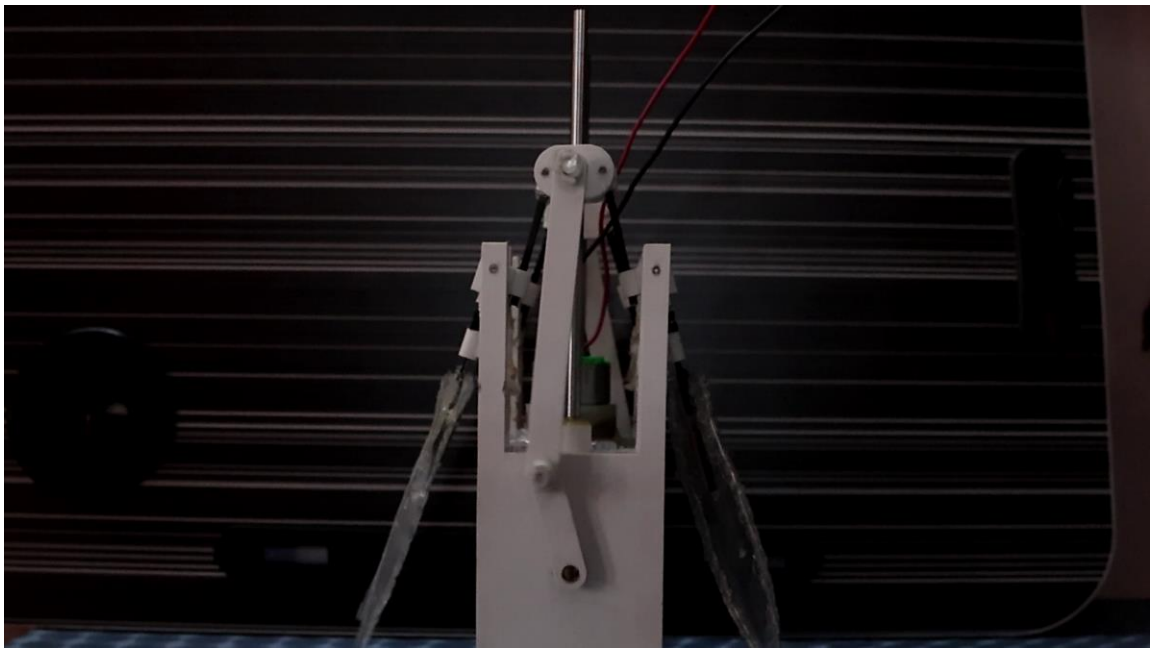

Fig 12 (Max negative angular amplitude position)

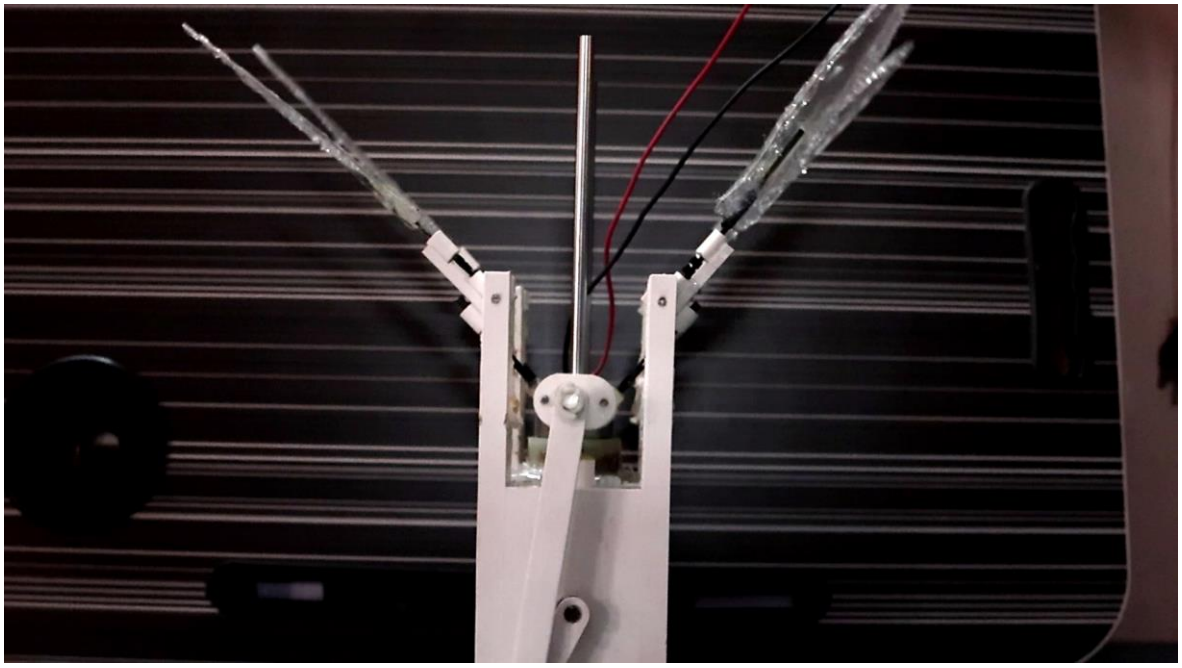

Fig 13 (Max positive angular amplitude position)

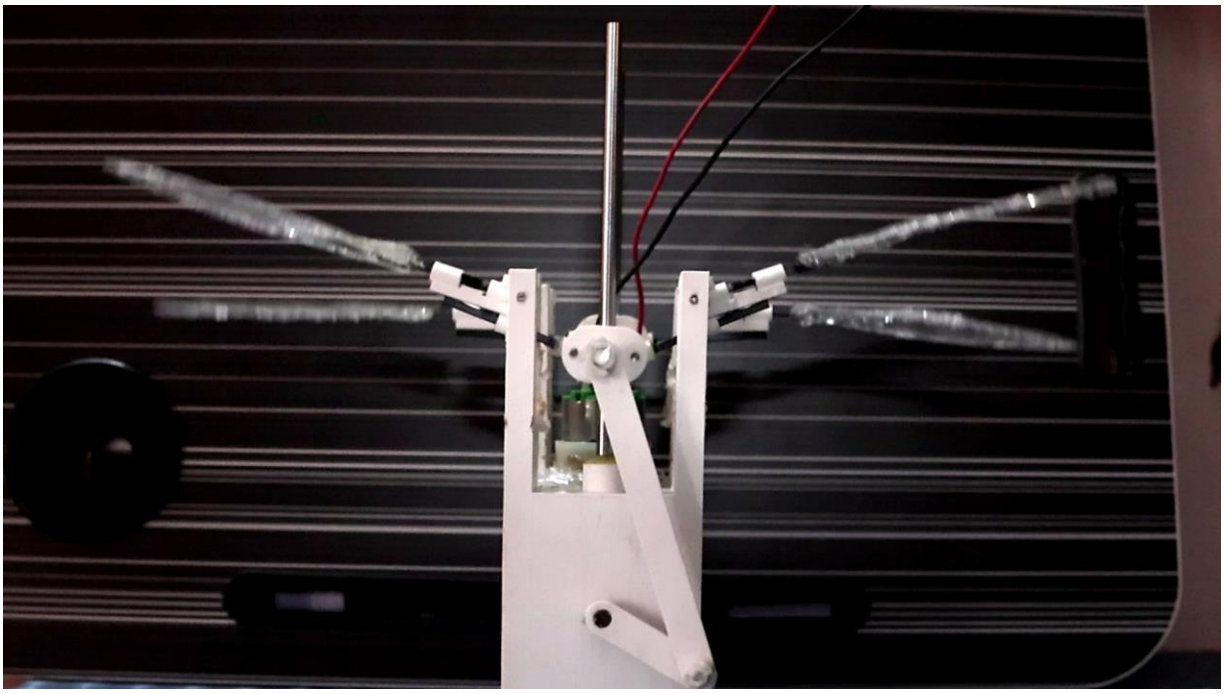

Fig 14 (Intermediate position during upstroke)

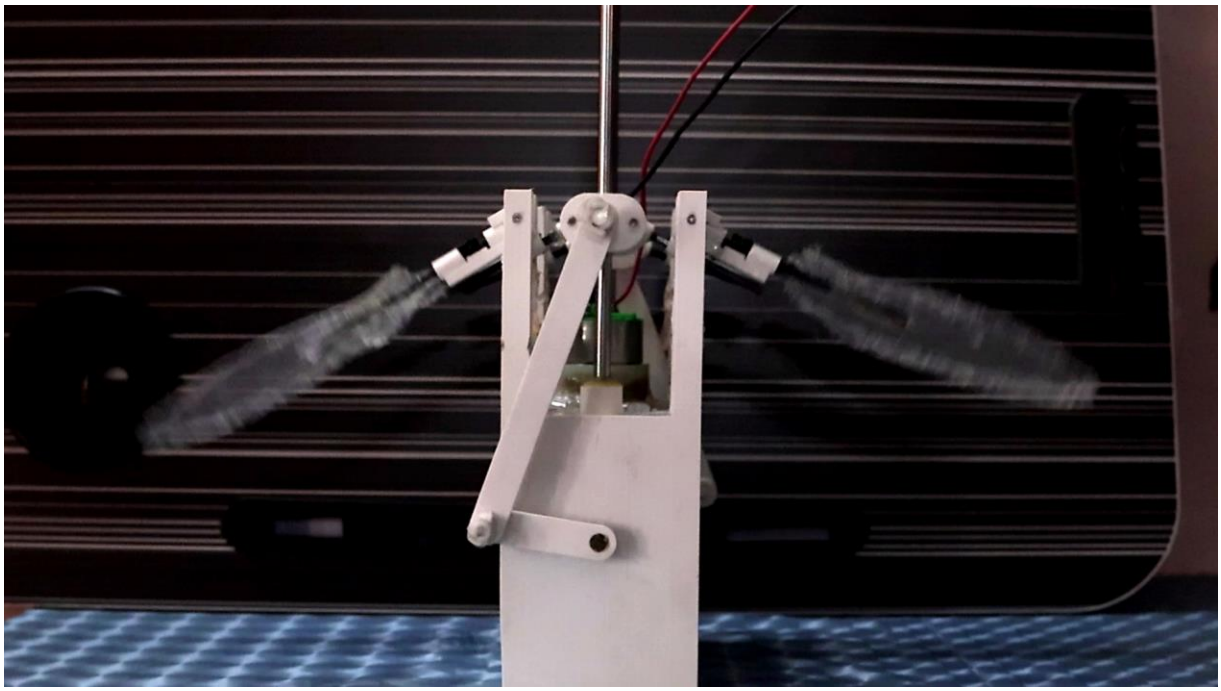

Fig 15 (Intermediate position during downstroke)

The model effectively emulates the flapping motion observed in dragonflies. Notably, when the initial phase is set to zero, the two extremities of the oscillatory motion and the downstroke reveal that the fore and hind wings exhibit zero phase difference. In an

intermediate position during the upstroke, a slight phase disparity is evident between the fore and hind wings, with the hind wings demonstrating slightly lower angular velocity. This discrepancy can be attributed to the unequal down forces experienced by the wing pairs during the upstroke due to variations in wing area. During the downstroke, gravitational forces take precedence, and the aerodynamic force difference between the fore and hind wings becomes negligible. Hence the zero phase difference.

Down force measurements are taken at a wingbeat frequency of about 2 Hz and an initial phase difference of 0^{o}.

	Timestamp (s)	Force (N)
Before Flapping	10.373	4.879143
	11.487	4.975116
	11.487	4.975116
	12.624	4.879143
	13.716	4.926832
After Flapping	18.958	6.24007
	19.187	6.22439
	19.367	6.316186
	19.511	6.24023
	20.92	6.24007
	21.13	5.997202
	21.333	6.25024

The following plot is obtained on analysis of force readings with time.

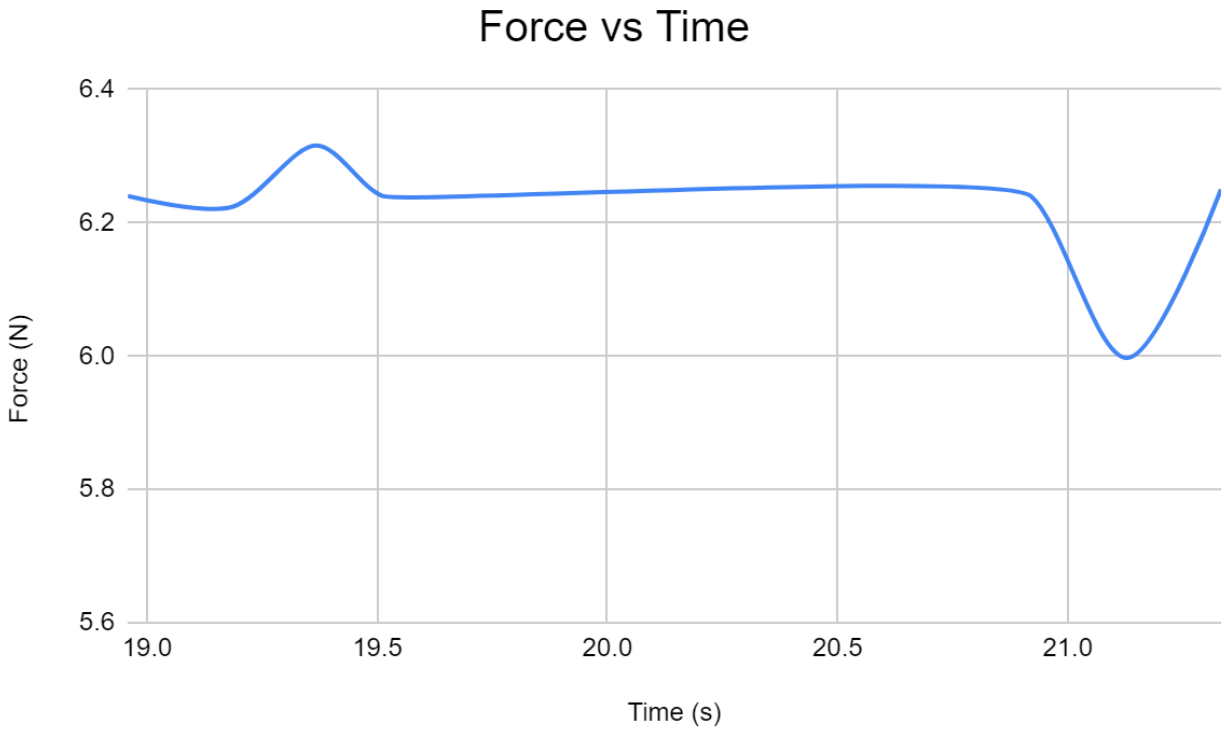

The depicted plot displays both maximum and minimum force values. Since the force sensor that we have used does not respond to the changes in force fast enough, we have to resort to some form of heuristic method for the calculation of lift from the slow reacting sensor data. It's reasonable to infer that the minimum force occurs during the downstroke, given the reduced downforce associated with a slight lift force during this phase. Conversely, the maximum force can be assumed to transpire during the upstroke, attributed to an increased downforce resulting from air resistance during the upward motion. The difference between these two values can be considered a suitable equivalent proportional to the lift force.

It is also observed that the force increase during the upstroke is notably less pronounced than the force reduction in the downstroke. This phenomenon is attributed to passive rotation. In the downstroke, the wing aligns almost parallel to the ground, causing the air force to act perpendicularly. However, during the upstroke, the wing's angle with the ground results in only a component of the force being perpendicular. Consequently, the upstroke exhibits a milder force increase compared to the more substantial force decrease observed in the downstroke.

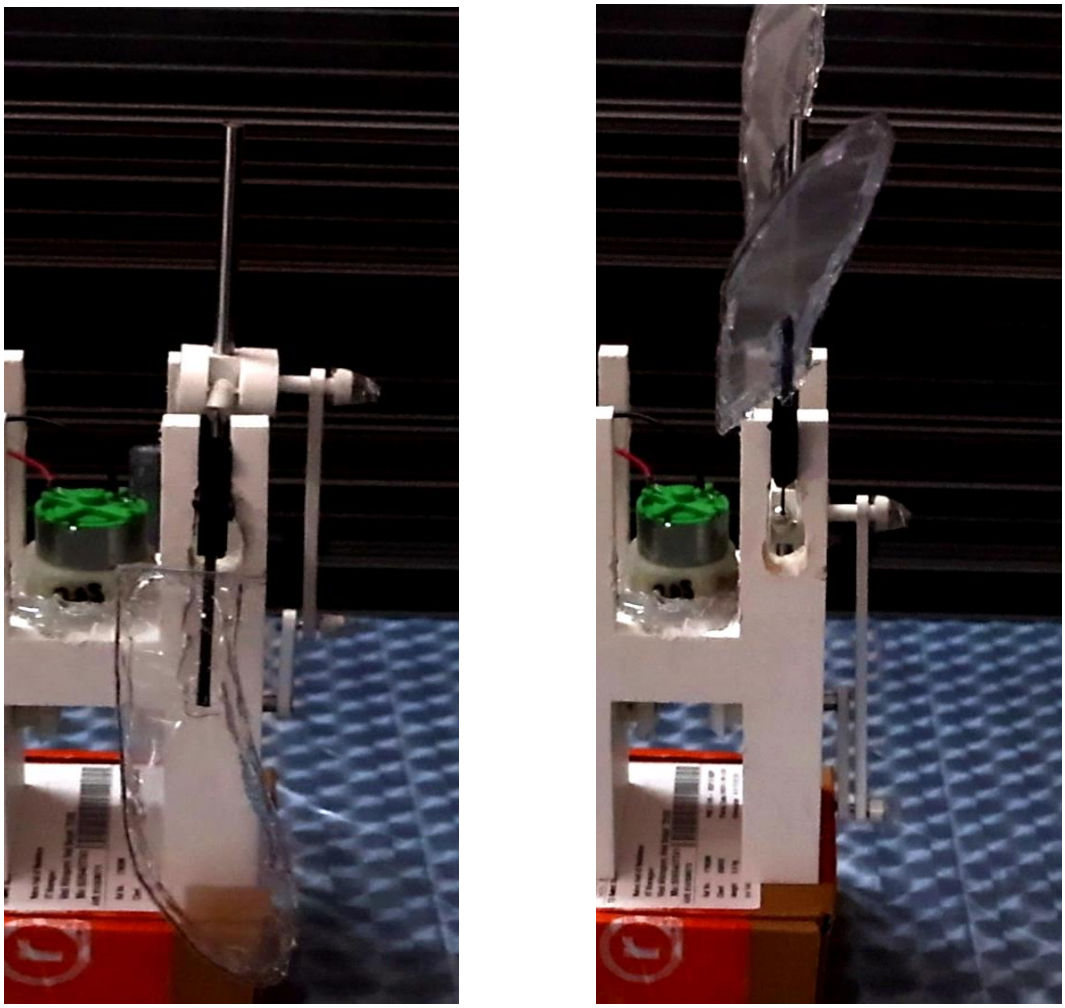

Fig 16 (Passive rotation motion)

Smoke Flow Visualization:

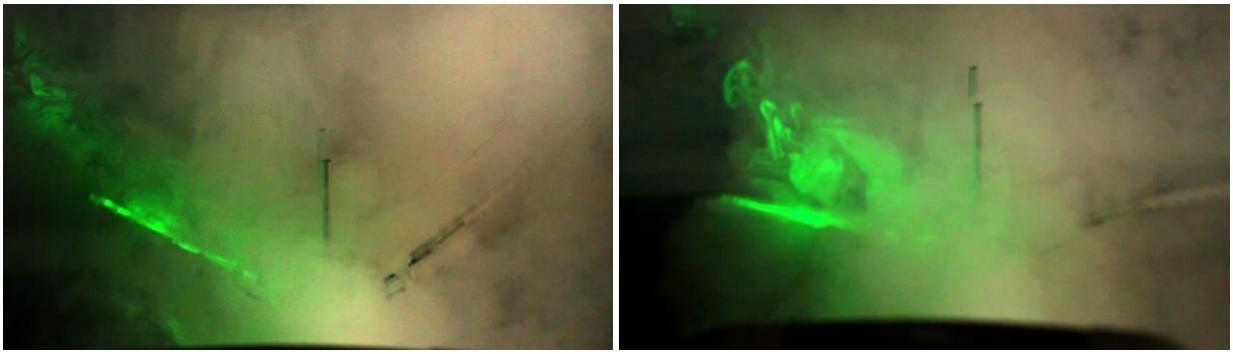

Fig 17 (Front View, Smoke Flow Visualization)

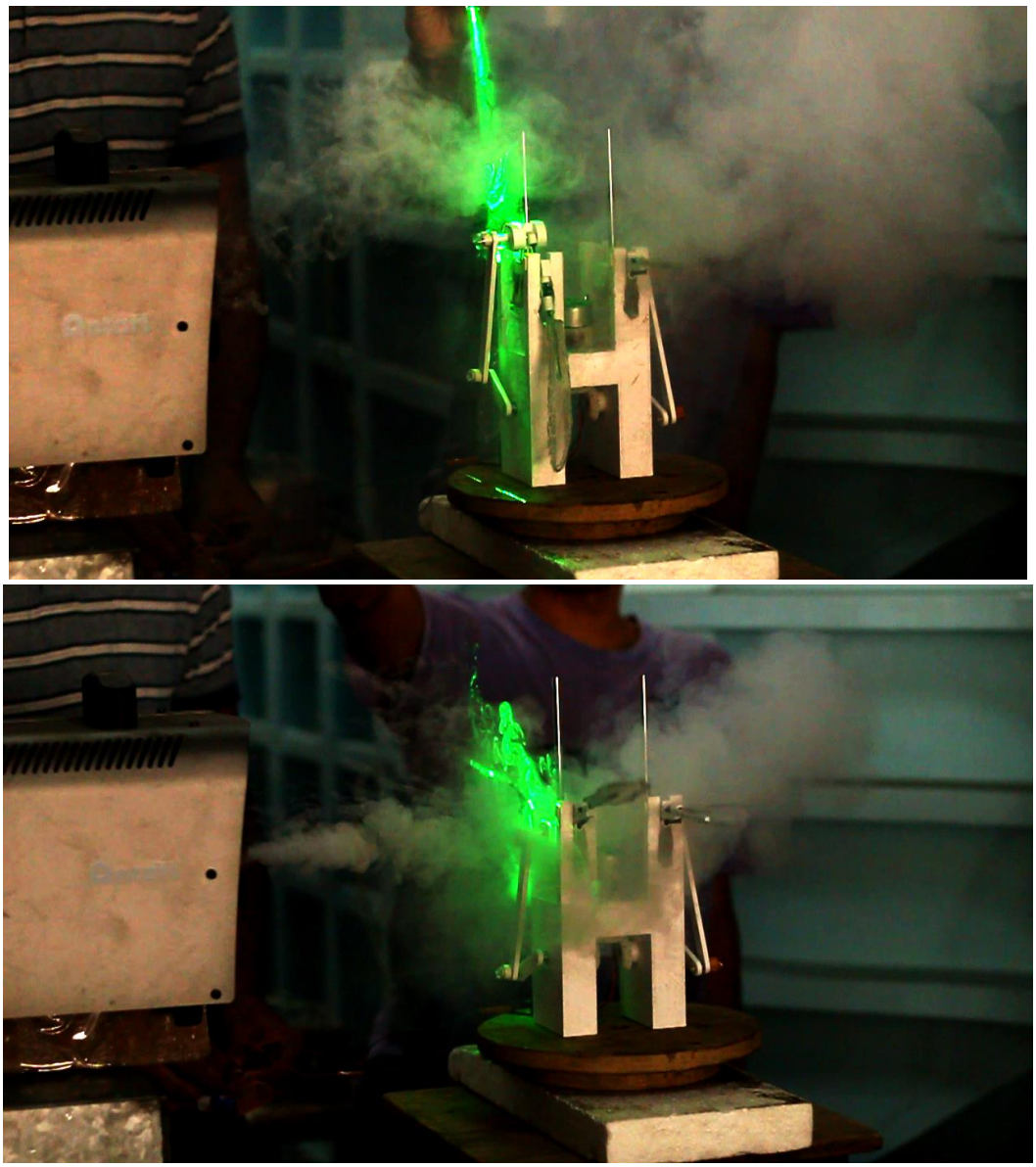

Fig 18 (Alternative View, Smoke Flow Visualization)

The generated smoke flow exhibited turbulence, prompting an examination of how the turbulent flow field was influenced by the flapping wings. The flow field displayed a combination of small and large eddies. Due to the high turbulence, no qualitative deductions were drawn. The presented visualization offers a comprehensive portrayal of the intricate dynamics involved in the flapping motion of dragonfly wings within a turbulent environment. The turbulent nature of the environment adds an additional layer of complexity to the visual representation, emphasizing the challenges and complexities associated with studying the aerodynamics of flapping wings in real-world, dynamic conditions.

FUTURE WORK

- Including a mechanism that allows us to change the phase difference between the forewing and hindwing, and compare the lift in each case.
- Implementing varied speeds during the upstroke and downstroke by employing a cam mechanism.
- Analyze the lift enhancement due to interaction of vortices between forewing and hindwing.
- Prepare a proper mount for the 3D model and test it in the wind tunnel.

INDIVIDUAL CONTRIBUTION:

Link for individual contribution statements by group members:
https://drive.google.com/drive/folders/1La2pB2OkSST9scm4otHIo0iQpDt4uT_U?usp=drive_link

REFERENCES:

[1] D. Alexander, "Unusual phase relationships between the forewing and hindwings in flying dragonflies," Journal of Experimental Biology

[2] S. P. Sane and M. H. Dickinson, "The control of flight force by a flapping wing: Lift and drag production," Journal of Experimental Biology

[3] Wakeling and C. Ellington, "Dragonfly flight I. gliding flight and steady-state aerodynamic forces," Journal of Experimental Biology

[4] Wang ZJ and Russell D. Effect of forewing and hindwing interactions on aerodynamic forces and power in hovering dragonfly flight. Phys Rev Lett 2007; 99: 148101.

[5] Sun M and Huang H. Dragonfly forewing-hindwing interaction at various flight speeds and wing phasing. AIAA J 2007; 45: 508–511.

[6] "Design and Experiments of a Dragonfly Inspired Robot" by Christopher DiLeo and Xinyang Deng

[7] Wang ZJ. Two dimensional mechanism for insect hovering. Phys Rev Lett 2000; 85: 2216.

[8] Weis-Fogh T. Quick estimates of flight fitness in hovering animals, including novel mechanisms for lift production. J Exp Biol 1973; 59: 169–230.

APPENDIX:

CAD Models:
https://drive.google.com/drive/folders/1zkzQJ1BmZcqH0szUY2JIuBF0DqD-vq0J?usp=sharing

Demo Video and Smoke Flow visualization Video:
https://drive.google.com/drive/folders/1l26BtkaTKktjHgPLjE71wCp7ybETEWGa?usp=drive_link

Force Measurement datasheet:
https://docs.google.com/spreadsheets/d/1Kj0k255hGiO4cKwZrtMb0EC6sE2ErDpWWj2aFspfnh4/edit?usp=sharing

GROUP MEMBERS:

1) Aswin D Menon (21AE10044)
2) Rahul Sunil (21AE10050)
3) Adithyan U S (21AE10049)
4) Anfal S (21AE10003)
5) Sagar K P (21AE30031)
6) Allwin Johnjo Prince (21AE10002)
7) Arjun Biju (21AE10007)
8) Nikhith Mathai Manoj (21AE10027)
9) Bhanupriya Gupta (21AE10011)